Journal of Hydrology, 146 (1993) 421–449
Elsevier Science Publishers B.V., Amsterdam

[4]

Floodflow frequency model selection in Australia

Richard M. Vogel[a], Thomas A. McMahon[b] and Francis H.S. Chiew[b]

[a]*Department of Civil and Environmental Engineering, Tufts University, Medford, MA 02155, USA*
[b]*Department of Civil and Agricultural Engineering, University of Melbourne, Parkville, Vic. 3052, Australia*

(Received 30 April 1992; accepted 7 September 1992)

ABSTRACT

Vogel, R.M., McMahon, T.A. and Chiew, F.H.S., 1993. Floodflow frequency model selection in Australia. J. Hydrol., 146: 421–449.

Uniform flood frequency guidelines in Australia and the United States recommend the use of the log Pearson type 3 (LP3) distribution in flood frequency investigations. Many investigators have suggested alternate models such as the Generalized Extreme Value (GEV) distribution as an improvement over the LP3 distribution. Using floodflow data at 61 sites across Australia, we explore the suitability of various flood frequency models using *L*-moment diagrams. We also repeat the experiment performed in the original US Water Resource Council report (Bulletin 17B) which led to the LP3 mandate in the United States. Our evaluations reveal that among the models tested, the GEV and Wakeby distributions provide the best approximation to floodflow data in the regions of Australia that are dominated by rainfall during the winter months, such as southwest Western Australia and Tasmania. For the remainder of the continent, the Generalized Pareto (GPA) and Wakeby distributions provide the best approximation to floodflow data. The two- and three-parameter log-normal models and the LP3 distribution performed satisfactorily, yet not as well as either the GEV or GPA distributions. Other models such as the Gumbel, log--normal, normal, Pearson, exponential, and uniform distributions are shown to perform poorly. Recent research indicates that regional index-flood type procedures should be more accurate and more robust than the type of at-site procedures evaluated here. Nevertheless, this study reveals that index-flood procedures should not be restricted to a single distribution such as the GEV distribution because other distributions such as the GPA distribution perform significantly better in the most densely populated regions of Australia.

INTRODUCTION

Many innovations in the field of flood frequency analysis have occurred since the decision of the Institution of Engineers (Pilgrim, 1987) and the US Water Resources Council (1967) to recommend the use of the log Pearson type 3 (LP3) distribution for floodflow investigations in Australia and the United States, respectively. The state of the art of selecting a regional flood

Correspondence to: R.M. Vogel, Department of Civil and Environmental Engineering, Tufts University, Medford, MA 02155, USA.

0022-1694/93/$06.00

frequency distribution around the time of the LP3 mandate in the United States was considerably different from the current situation. For example, in describing the US Water Resource Council (WRC) Work Group study (1967), Benson (1968) argued that 'no single method of testing (alternate hypotheses) was acceptable to all those on the Work Group, and the statistical consultants could not offer a mathematically rigorous method' leading to the conclusion that 'there are no rigorous statistical criteria on which to base a choice of method'.

More recently, *L*-moment diagrams and associated goodness-of-fit procedures (see e.g. Wallis, 1988; Cunnane, 1989; Hosking, 1990; Nathan and Weinmann, 1991; Chowdhury et al., 1991; Pearson et al., 1991; Pearson, 1992; Vogel et al., 1993) have been advocated for evaluating the suitability of selecting various distributional alternatives for modeling floodflows in a region. For example, Wallis (1988, fig. 3) found an *L*-moment diagram useful for rejecting Jain and Singh's (1987) conclusion that annual maximum floodflows at 44 sites were well approximated by a Gumbel distribution and for suggesting a GEV distribution instead. Vogel et al. (1993) used *L*-moment diagrams to show that the two- and three-parameter log–normal models (LN2 and LN3), the LP3 and the GEV distributions were all acceptable models of floodflows in the southwestern United States.

A second approach for evaluating the fit of alternate probability models and associated parameter estimation schemes is that of non-parametric experiments of the type performed by Beard (1974) and summarized by the Interagency Advisory Committee on Water Data (IACWD) (1982, appendix 14) and more recently by Gunasekara and Cunanne (1992). Using 300 stations distributed across the entire USA, Beard counted the number of stations for which the estimated 1000 year floodflow was exceeded in the historical record. Eight independent methods were employed for estimating the 1000 year flood at each site. Beard argued that with a total of $n = 14,200$ station-years of data across the 300 sites, one would expect approximately 14 exceedances of the true 1000 year floodflow. Only the LP3 and LN2 distributions came close to reproducing the 14 expected exceedances. Beard (1974) performed many other tests, but it was this test which convinced hydrologists that both the LP3 and LN2 models approximate the distribution of observed floodflow data throughout the entire US.

Another approach to evaluating the fit of alternate probability models to a regional database is to employ probability plots and associated probability plot correlation coefficient (PPCC) tests (Vogel, 1986; Vogel and Kroll, 1989; Vogel and McMartin, 1991; Chowdhury et al., 1991). Since PPCC hypothesis tests are best suited for use with two-parameter distributions, and floodflows usually

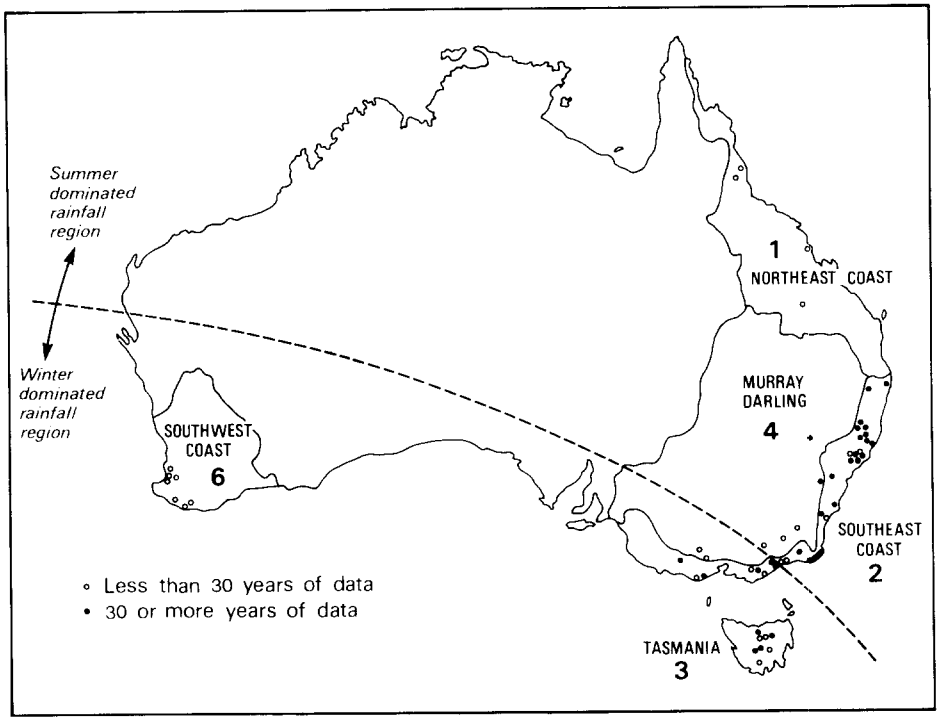

Fig. 1. Location map of basins used in this study. The dashed line separates the continent into two broad hydrologic regimes. The region above the dashed line is dominated by rainfall during summer months and the region below the dashed line is dominated by rainfall during winter months.

require three-parameter distributions, we do not consider PPCC tests here.

In the following sections, we employ *L*-moment diagrams and Beard's non-parametric test to annual maximum floodflow data in Australia. Our goal is to assess the adequacy of various flood frequency procedures and to choose plausible procedures for approximating the underlying distribution of floodflows for this continent.

STUDY REGION

The annual maximum floodflow data employed in this study include 61 gauging stations with unregulated streamflow record lengths of 20 or more years. Of those 61 stations, there are 32 with record lengths of 30 or more years. These stations are located across portions of the continent of Australia as shown in Fig. 1. The station numbers, river names, periods of record, record lengths and drainage areas are summarized in Table 1. To aid in future comparisons we refer to each of the major drainage divisions shown in Fig.

TABLE 1

Streamflow gauging stations and L-moments of annual instantaneous peak flow data

Streamflow gauging station	Catchment area (km^2)	Period of data (years of record)	L-C_v τ_2	L-skew τ_3	L-kurtosis τ_4
Northeast coast					
111105 Babinda Creek at the Boulders	39	1967–1989 (22)	0.264	0.112	0.068
113004 Cochable Creek at Powerline	93	1967–1989 (23)	0.376	0.419	0.347
120204 Broken River at Crediton	41	1956–1987 (32)	0.446	0.138	0.038
130503 Carnavon Creek at Wyseby Station	570	1967–1987 (21)	0.404	0.141	0.064
Southeast coast					
203002 Coopers Creek at Repentance	62	1921–1990 (40)	0.371	0.156	0.067
204006 Bookookoorara River at Undercliffe	127	1922–1982 (22)	0.646	0.584	0.391
204008 Guy Fawkes River at Ebor	31	1924–1990 (40)	0.503	0.404	0.254
204017 Bielsdown Creek at Dorrigo	82	1948–1990 (38)	0.435	0.305	0.165
204025 Orara River at Karangi	135	1926–1990 (37)	0.339	0.173	0.019
204036 Cataract Creek at Sandy Hill	236	1952–1990 (38)	0.531	0.408	0.174
206001 Styx River at Jeogla	163	1919–1991 (72)	0.526	0.394	0.175
206009 Tia River at Tia	261	1928–1990 (60)	0.550	0.431	0.178
206010 Yarrowitch River at Yarrowitch	70	1929–1984 (48)	0.519	0.394	0.210
208001 Barrington River at Bob's Crossing	20	1945–1989 (24)	0.372	0.399	0.205
208009 Barnard River at Barry	150	1950–1991 (30)	0.432	0.320	0.188
210011 Williams River at Tilligra	194	1932–1986 (45)	0.443	0.228	0.055
210017 Moonan Brook at Moonan Brook	103	1941–1988 (40)	0.465	0.383	0.175
210022 Allyn River at Halton	205	1941–1990 (42)	0.380	0.194	0.137
210026 Congewai Creek at Eglinford	83	1949–1978 (26)	0.334	−0.192	−0.058
212008 Cox River at Bathurst Road	199	1951–1989 (34)	0.623	0.485	0.289
214003 Macquarie Rivulet at Albion Park	35	1950–1990 (33)	0.624	0.464	0.239
215004 Corang River at Hockeys	166	1925–1990 (61)	0.429	0.273	0.161
215006 Mongarlowe River at Mongarlowe	130	1950–1980 (21)	0.349	0.049	0.148

TABLE 1 (continued)

Streamflow gauging station	Catchment area (km^2)	Period of data (years of record)	L-C_v τ_2	L-skew τ_3	L-kurtosis τ_4
218001 Turros River at Turros Vale	93	1949–1990 (30)	0.432	0.122	0.028
219001 Rutherford Creek at Brown Mountain	15	1949–1990 (41)	0.528	0.298	0.118
219006 Tantawanglo Creek at Tantawanglo Mountain	88	1952–1989 (38)	0.557	0.376	0.196
221201 Cann River (West Branch) at Weeragua	311	1958–1990 (31)	0.450	0.204	0.125
222213 Suggan Buggan River at Suggan Buggan	357	1958–1989 (32)	0.460	0.303	0.134
223204 Nicholson River at Deptford	293	1963–1990 (28)	0.473	0.136	−0.056
223205 Tambo River D/S Ramrod Creek	2681	1966–1987 (22)	0.502	0.238	0.045
224203 Mitchell River at Glenaladale	3903	1961–1990 (30)	0.443	0.344	0.164
224206 Wonnangatta River at Crooked River	1096	1954–1989 (32)	0.378	0.164	0.064
225208 Thomson River at Cooper Creek	906	1970–1990 (21)	0.604	0.586	0.384
226220 Loch River at Noojee	97	1963–1989 (27)	0.322	0.434	0.322
227219 Bass River at Loch	52	1967–1990 (24)	0.317	0.308	0.246
228207 Bunyip River at Headworks	41	1951–1987 (37)	0.338	0.133	0.030
233214 Barwon River (East Branch) at Forrest	17	1956–1990 (35)	0.514	0.328	0.122
235205 Arkins River (West Branch) at Wyelangta	90	1960–1990 (29)	0.501	0.586	0.442
238208 Jimmy Creek at Jimmy Creek	23	1951–1990 (36)	0.427	0.231	0.171
Tasmania					
3040089 Nive River at Gowan Brae	185	1965–1991 (27)	0.197	0.280	0.202
3070001 Davey River D/S Crossing River	686	1966–1991 (25)	0.175	0.227	0.137
3080003 Franklin River at Mount Fincham Track	757	1954–1991 (37)	0.160	0.165	0.117
3090001 King River at Crotty	449	1949–1990 (42)	0.200	0.307	0.281
3100010 Que River below Bulgobac Creek	119	1964–1991 (28)	0.202	0.297	0.168
3120001 Hellyer River at Guildford Junction	102	1923–1991 (64)	0.193	0.256	0.228

TABLE 1 (continued)

Streamflow gauging station	Catchment area (km^2)	Period of data (years of record)	L-C_v τ_2	L-skew τ_3	L-kurtosis τ_4
3150006 Forth River above Lemonthyme	311	1963–1990 (28)	0.214	0.359	0.344
3180028 South Esk above Macquarie River	3280	1957–1990 (34)	0.464	0.400	0.218
Murray–Darling					
401212 Nariel Creek at Upper Nariel	252	1935–1981 (29)	0.274	0.204	0.112
403218 Dandongadale River at Matong North	182	1963–1989 (26)	0.460	0.449	0.379
407214 Creswick Creek at Clunes	308	1965–1990 (25)	0.358	0.021	0.010
408202 Avoca River at Amphitheatre	78	1967–1991 (24)	0.465	0.193	0.008
410534 Happy Jacks River above Happy Jacks Pondage	109	1961–1982 (22)	0.545	0.650	0.536
420003 Belar Creek at Warkton	133	1952–1989 (34)	0.579	0.455	0.244
421034 Slippery Creek at Dam Site	15	1955–1988 (31)	0.575	0.472	0.251
Southwest coast					
606185 Shannon River at Dog Pool	350	1965–1990 (21)	0.286	0.128	0.232
606195 Weld River at Ordnance Road Crossing	240	1965–1990 (22)	0.243	0.332	0.265
607155 Dombakup Brook at Malimup Track	114	1963–1990 (21)	0.397	0.395	0.205
613109 Samson Brook below Dam	62	1960–1989 (21)	0.434	0.432	0.293
614016 North Dandalup River at Scarp Road	153	1962–1990 (24)	0.274	0.226	0.093
614044 Yarragil Brook at Yarragil Formation	73	1959–1990 (24)	0.352	0.217	0.183
614047 Davies Brook at Murray Valley Plantations	67	1960–1989 (21)	0.361	0.462	0.386

1 and Table 1 using the first number in the station number. Regions 1, 2, 3, 4 and 6 correspond to the northeast coast, southeast coast, Tasmania, Murray–Darling and southwest drainage divisions, respectively. Note that the highest density of streamgauges is coincident with the highest population densities in the southeast coast (region 2). Overall, the density of streamgauges employed here can be considered to reflect the importance of the regions, in terms of population, economy and agriculture. The southeast region (region

2) is by far the most densely populated region and the Murray–Darling region (region 4) is the most important agricultural region.

No significant withdrawals, diversions or other regulating structures are contained in these basins; hence we consider the streamflows to be essentially unregulated. Overall, Australia is divided into 12 drainage basins. Of these, seven do not have a single stream with 20 or more years of data. The eight stations employed in Tasmania (region 3) and the seven on the southwest coast are the only stations in those regions with 20 or more years of record. There are more stations in the northeast coast (region 1), the Murray–Darling (region 4) and the southeast coast (region 2), that were not employed because information regarding their degree of regulation is not readily available.

THE METHOD OF *L*-MOMENTS

L-moments and probability weighted moments (PWMs) are analogous to ordinary moments in that their purpose is to summarize theoretical probability distributions and observed samples. Similar to ordinary product moments, *L*-moments can also be used for parameter estimation, interval estimation and hypothesis testing. Although the theory and application of *L*-moments parallels that for conventional product moments, *L*-moments have several important advantages. Since sample estimators of *L*-moments are always linear combinations of the ranked observations, they are subject to less bias than ordinary product moments. This is because ordinary product-moment estimators such as the sample variance and sample skew coefficient, require squaring and cubing the observations, respectively, which causes them to give greater weight to the observations far from the mean, resulting in substantial bias and variance (Wallis et al., 1974). Hosking (1990) and Stedinger et al. (1993) provide a summary of the theory and application of *L*-moments. Greenwood et al. (1979) summarize the theory of PWMs.

Perhaps the simplest approach to describing *L*-moments is by first defining probability weighted moments (PWMs) because *L*-moments are linear functions of PWMs (Greenwood et al., 1979; Hosking, 1990). PWMs may be defined by

$$\beta_r = E\{X[F_X(x)]^r\} \tag{1}$$

where β_r is the rth order PWM and $F_X(x)$ is the cdf of X. When $r = 0$, β_0 is the mean streamflow. Hence a sample estimate of the first PWM, which we term b_0 is simply the sample mean. All higher order PWMs are linear combinations of the order statistics $X_{(n)} \leqslant, \ldots, \leqslant X_{(1)}$.

Landwehr et al. (1979) recommend the use of biased estimates of PWMs and *L*-moments, since such estimators often produce quantile estimates with

lower root mean square error than unbiased alternatives. Nevertheless, unbiased estimators are often preferred in goodness-of-fit evaluations such as L-moment diagrams (see Stedinger et al., 1993). Unbiased sample estimates of the PWMs, for any distribution can be computed from

$$b_0 = \frac{1}{n}\sum_{j=1}^{n} x_j \tag{2a}$$

$$b_1 = \sum_{j=1}^{n-1}\left[\frac{(n-j)}{n(n-1)}\right]x_{(j)} \tag{2b}$$

$$b_2 = \sum_{j=1}^{n-2}\left[\frac{(n-j)(n-j-1)}{n(n-1)(n-2)}\right]x_{(j)} \tag{2c}$$

$$b_3 = \sum_{j=1}^{n-3}\left[\frac{(n-j)(n-j-1)(n-j-2)}{n(n-1)(n-2)(n-3)}\right]x_{(j)} \tag{2d}$$

where $x_{(j)}$ represents the ordered streamflows with $x_{(1)}$ being the largest observation and $x_{(n)}$ the smallest. The PWM estimators in eqn. (2) can be more generally described using

$$b_r = \frac{1}{n}\sum_{j=1}^{n-r}\left[\frac{\binom{n-j}{r}}{\binom{n-1}{r}}\right]x_{(j)} \tag{3}$$

For any distribution, the first four L-moments are easily computed from the PWMs using

$$\lambda_1 = \beta_0 \tag{4a}$$

$$\lambda_2 = 2\beta_1 - \beta_0 \tag{4b}$$

$$\lambda_3 = 6\beta_2 - 6\beta_1 + \beta_0 \tag{4c}$$

$$\lambda_4 = 20\beta_3 - 30\beta_2 + 12\beta_1 - \beta_0 \tag{4d}$$

The first four unbiased L-moment sample estimators are obtained by substituting the PWM sample estimators b_r, from eqn. (2) into the L-moment equations in eqn. (4). Equations (4a)–(4d) are special cases of the general recursion

$$\lambda_{r+1} = \sum_{k=0}^{r}\beta_r(-1)^{r-k}\binom{r}{k}\binom{r+k}{k} \tag{5}$$

A generalized computer program is available for implementing the method of L-moments for a wide range of commonly used distributions (Hosking,

1991b). In the following sections we briefly define L-moment ratios, discuss their relationship to conventional moments and introduce L-moment diagrams.

L-*moment ratios and the interpretation of* L-*moments*

Analogous to the product moment ratios; coefficient of variation $C_v = \sigma/\mu$, skewness γ and kurtosis κ, Hosking (1990) defines the L-moment ratios

$$\tau_2 = \frac{\lambda_2}{\lambda_1} \equiv L\text{-coefficient of variation} \tag{6a}$$

$$\tau_3 = \frac{\lambda_3}{\lambda_2} \equiv L\text{-skewness} \tag{6b}$$

and

$$\tau_4 = \frac{\lambda_4}{\lambda_2} \equiv L\text{-kurtosis} \tag{6c}$$

where λ_r, $r = 1, ..., 4$ are the first four L-moments and τ_2, τ_3 and τ_4 are the L-coefficient of variation (L-C_v), L-skewness and L-kurtosis, respectively. The first L-moment λ_1 is equal to the mean streamflow μ, hence it is a measure of location. Hosking (1990) shows that λ_2, τ_3 and τ_4 can be thought of as measures of a distribution's scale, skewness and kurtosis, respectively, analogous to the ordinary moments σ, γ and κ, respectively.

L-*moment diagrams*

An L-moment diagram compares sample estimates of the dimensionless ratios τ_2, τ_3, τ_4 with their population counterparts, for a range of assumed distributions. An advantage of L-moment diagrams is that one can compare the fit of several distributions using a single graphical instrument. Figure 2 compares the theoretical relationships between L-kurtosis and L-skewness for the exponential, uniform, normal, Gumbel, GEV, three-parameter log-normal (LN3), Pearson type 3 (P3), lower bound of a Wakeby (WA5) and the GPA distributions. Figure 2 is a plot of L-moments of streamflow in real space, hence it is not possible to represent the log Pearson type 3 (LP3) distribution. We consider L-moment diagrams in log space for that purpose, later on.

Clearly the two-parameter distributions, which are defined by only a point in L-kurtosis–L-skewness space, do not have nearly the flexibility of their three-parameter versions. The line marked WA5 represents the lower bound of the L-kurtosis–L-skewness space which can be captured by the five-parameter Wakeby distribution. The Wakeby distribution is the most flexible

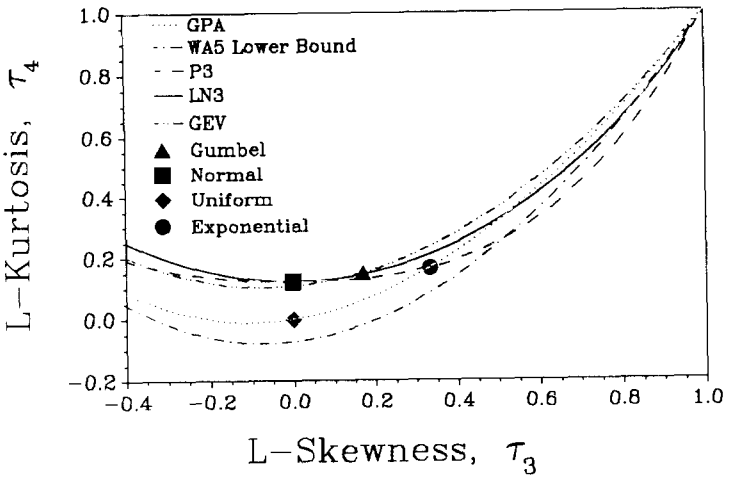

Fig. 2. Theoretical L-moment relationships for the exponential, uniform, normal, Gumbel, Generalized Extreme Value (GEV), log-normal (LN3), Pearson (P3), Generalized Pareto (GPA) distributions and the lower bound of the Wakeby distribution (WA5).

distribution considered since it defines a two-dimensional region in Fig. 2 rather than a line or a point as is the case for the three- and two-parameter distributions, respectively. Figure 2 was constructed using the polynomial approximations developed by Hosking (1991a) and summarized by Stedinger et al. (1993).

L-MOMENT DIAGRAMS FOR AUSTRALIAN FLOODFLOWS

Figure 3 compares the relationship between sample estimates of τ_4 and τ_3 (using circles) and their population values for the 61 stations in Australia. Here sample estimates of τ_2, τ_3 and τ_4 are obtained using the probability weighted moment estimators of λ_1, λ_2, λ_3 and λ_4 as recommended by Stedinger et al. (1993), when constructing L-moment diagrams. Unbiased probability weighted moment estimators are equivalent to the unbiased L-moment estimators introduced by Hosking (1990). Note that use of unbiased estimators of the sample L-moments λ_r, $r = 1, ...4$, does not imply that the L-moment ratio estimators τ_i, $i = 1, 2$, and 3, are unbiased. Figure 3(a) was constructed using annual maximum floodflow data for the 61 Australian basins with record lengths greater than or equal to 20 years. Since the sample estimates of L-kurtosis and L-skewness are extremely variable for small samples we drop the short-record sites in Fig. 3(b), which uses only 32 basins with record lengths greater than or equal to 30 years. Figure 3(b) eliminates some of the sampling variability in the estimated L-kurtosis and L-skewness, enabling us to better distinguish which probability models best represent the

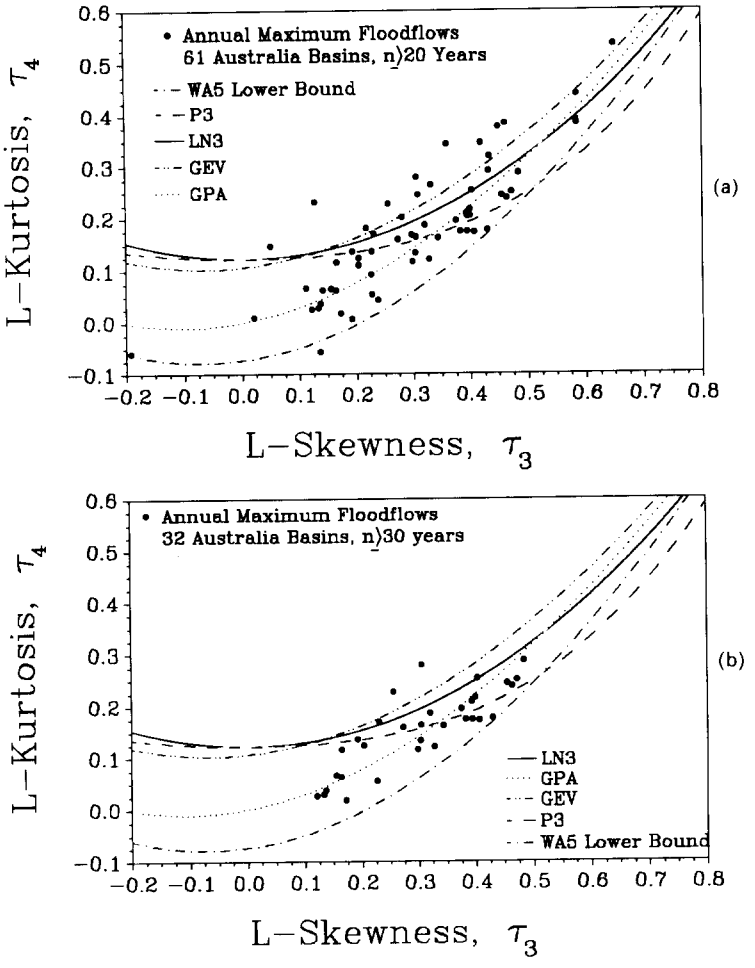

Fig. 3. L-moment diagrams comparing the sample and theoretical relationships between L-kurtosis and L-skewness for annual maximum floodflow data at (a) 61 Australian catchments with record lengths greater or equal to 20 years and (b) 32 Australian catchments with record lengths greater or equal to 30 years.

reduced data set. The true relationships between L-kurtosis and L-skewness corresponding to the P3, LN3, GEV, GPA and the lower bound of the WA5 distribution are shown for comparison in Fig. 3. Figures 3(a) and (b) reveal that, of the models tested, the GPA and Wakeby distributions appear to be most consistent with this entire regional sample. In both Figs. 3(a) and (b), roughly half the observations are above the GPA line and half below. None of the other two- or three-parameter distributions considered, approximate the behavior of this regional sample nearly as well as the GPA distribution. Since only one point in Fig. 3(a) falls below the Wakeby line, we also conclude

that a Wakeby distribution provides a good approximation to the distribution of floodflows in this region. However, since the Wakeby distribution requires estimation of five parameters, resulting quantile estimators are likely to perform poorly for the small samples normally encountered in flood frequency investigations.

Overall, there is significant variability in the L-moment ratio estimates illustrated in Fig. 3. Even though the GPA distribution appears to provide the best overall fit, the LN3 and GEV distributions also provide reasonable approximations to most of this regional sample.

In Fig. 4 we plot estimates of L-kurtosis and L-skewness of the logarithms of the annual maximum floodflows. For comparison we plot the theoretical relationship for P3 data which provides a test on whether the distribution of the logarithms of floodflow data resembles a P3 distribution, which is equivalent to checking whether the distribution of the floodflows resembles an LP3 distribution. Again, Fig. 4(a) uses the 60 basins (one basin was deleted since it had a zero floodflow) with record lengths greater or equal to 20 years and Fig. 4(b) uses the 32 basins with record lengths greater or equal to 30 years. We conclude that the LP3 distribution appears consistent with this regional sample of floodflows in Australia. McMahon and Srikanthan (1981) reached similar conclusions using ordinary product-moment diagrams. Using L-moment diagrams, Pearson et al. (1991) rejected the LP3 model in Western Australia, however their conclusions appear to be in error because their fig. 1 should have been labeled P3 rather than LP3, hence they should have rejected the P3 distribution not the LP3 distribution. In fact, Pearson et al. (1991) never tested the LP3 model.

Figure 5 illustrates the relationship between L-coefficient of variation (L-C_v) and L-skewness based on the 61 Australian basins. For comparison we plot, using a solid line, the theoretical relationship for the two-parameter GPA distribution. Again Figs. 5(a) and (b) compare the impact of dropping the sites with short records. When one drops the short-record sites, one observes in Fig. 5(b) that except for three sites, a two-parameter GPA distribution appears consistent with this regional sample. Here ξ, the third parameter in a GPA distribution is set to zero (see the Appendix). Since the GPA distribution has not been used commonly in hydrologic studies, we summarize its probability density function, cumulative density function and parameter estimation procedures in the Appendix. Hosking and Wallis (1987) provide an introduction to the GPA distribution and its use in flood frequency analysis.

From all our comparisons in Figs. 2, 3, 4 and 5, we conclude that the entire regional sample of annual maximum floodflows is reasonably well approximated by the GPA, LP3 and Wakeby probability distributions, marginally

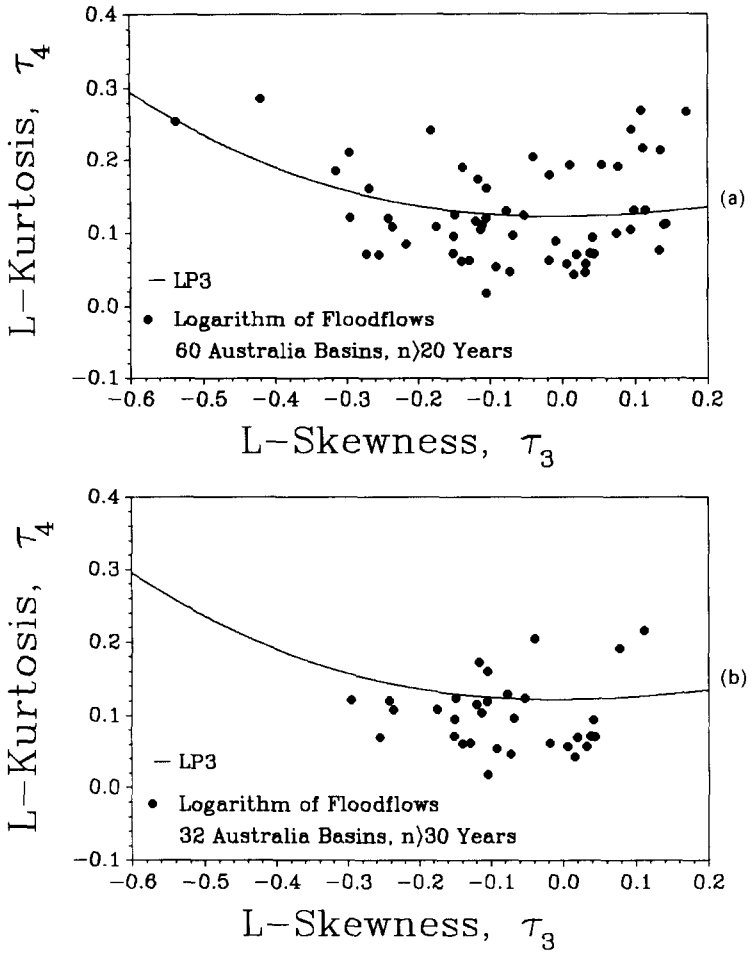

Fig. 4. *L*-moment diagrams comparing the sample and theoretical relationships between *L*-kurtosis and *L*-skewness for the logarithms of annual maximum floodflow data at (a) 60 Australian catchments with record lengths greater or equal to 20 years and (b) 32 Australian catchments with record lengths greater or equal to 30 years.

approximated by a GEV and LN3 distribution and poorly approximated by a P3, normal, exponential, uniform or Gumbel distribution.

Until now, we have attempted to choose a flood frequency model that can approximate the distribution of annual maximum floodflows for the entire continent of Australia. Since Australia exhibits a number of very different hydrologic and climatic regimes, it is informative to examine *L*-moment diagrams for selected homogeneous regions. The following sections reveal

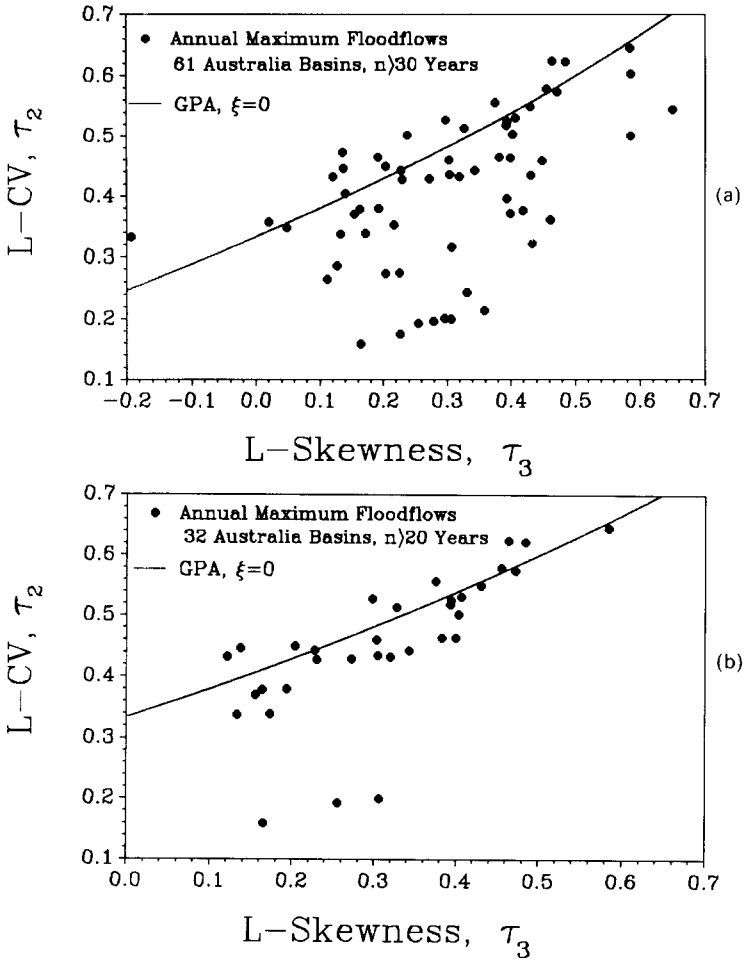

Fig. 5. *L*-moment diagrams comparing the sample and theoretical relationships between *L*-coefficient of variation and *L*-skewness for annual maximum floodflow data at (a) 61 Australian catchments with record lengths greater or equal to 20 years and (b) 32 Australian catchments with record lengths greater or equal to 30 years.

that separation of Australia into broad homogeneous regions can improve our ability to discriminate among potential flood frequency models.

Comparison with previous L-*moment studies*

Using *L*-moment diagrams, Pearson et al. (1991) concluded that annual maximum floodflows in the southwest coast (region 6) were well approximated by a GEV distribution. Pearson et al. (1991) used 28 basins with record lengths ranging from 10 to 36 years and an average length of only 18 years.

In our analysis, we elected to drop basins with record lengths of less than 20 years, hence we only employ seven basins in the southwest coast region of Australia.

Similarly Nathan and Weinmann (1991) used *L*-moment diagrams to evaluate alternative regional distributional hypotheses in central Victoria. Similar to Pearson et al. (1991) they concluded that annual maximum floodflows in the southwest portions of regions 2 and 4 are well approximated by a GEV distribution.

Pearson et al. (1991) and Nathan and Weinmann (1991) concluded that the GEV model best approximates the distribution of floodflows in southwest Western Australia, and central Victoria, respectively, yet our Fig. 3 documented that the GEV distribution performed poorly relative to the GPA distribution. This result suggests the need to define hydrologically homogeneous regimes for use in regional flood frequency analysis.

The dashed line in Fig. 1 separates the continent of Australia into two distinct rainfall regimes. The area below the dashed line receives most of its rainfall during the winter months, whereas the area above the dashed line receives most of its rainfall during the summer season. The entire Tasmania (region 3) and southwest coastal (region 6) regions are located within the winter-dominated rainfall zone. Similarly, most regions of central Victoria evaluated by Nathan and Weinmann (1991) fall within the winter-dominated rainfall zone. Approximately three quarters of the stations in the northeast coastal (region 1) and Murray–Darling regions (region 4) are located in the summer-dominated rainfall zones. However, half the stations are too close to the border separating the summer- and winter-dominated rainfall zones, for an accurate distinction to be made.

Figure 6 is an *L*-moment diagram based on only the eight sites in Tasmania (region 3) and the seven sites in the southwest coastal region (Region 6) which are subject to winter-dominated rainfall. Figure 6(a) reveals that the GEV distribution provides the best fit for the winter-dominated rainfall region. Roughly half the observations fall below the GEV line and half above it. This result supports the conclusions of both Pearson et al. (1991) and Nathan and Weinmann (1991), however neither of those investigators evaluated the GPA distribution.

In Fig. 6(b) we plot the observed values of L-C_v vs. L-skewness for the winter-dominated rainfall sites located in Tasmania (region 3) and the southwest coastal region (Region 6). This figure reveals that these sites are poorly approximated by a two-parameter GPA distribution and that these sites are exactly the sites which were outliers in Fig. 5(a). We conclude that the GEV distribution provides a good approximation to the distribution of

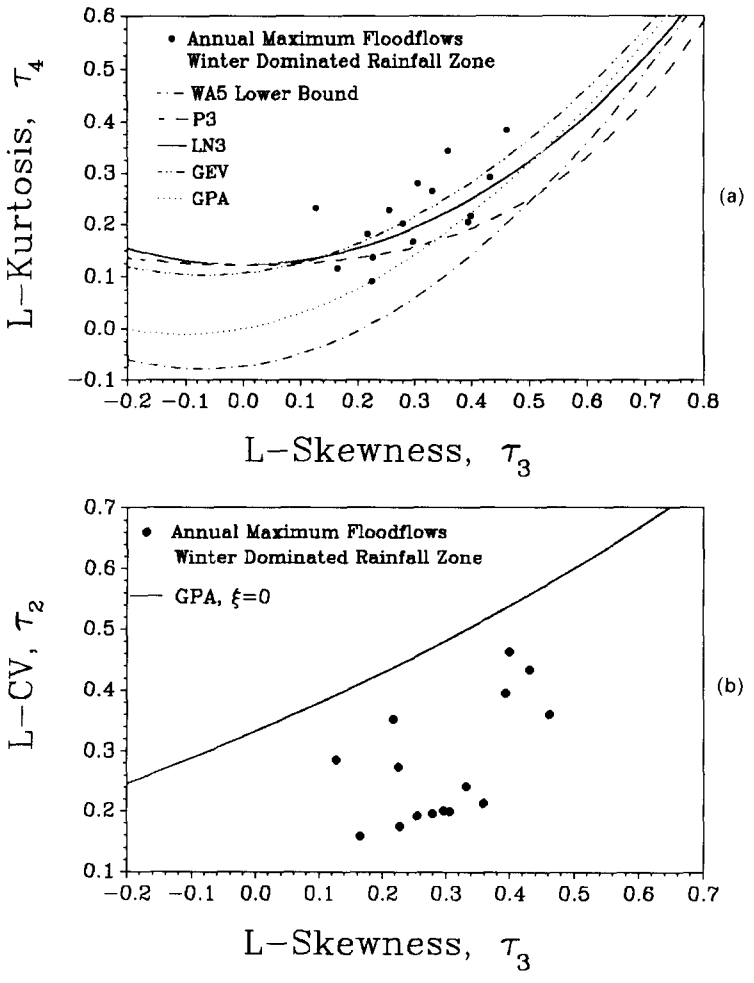

Fig. 6. *L*-moment diagrams comparing the sample and theoretical relationships between (a) *L*-kurtosis and *L*-skewness and (b) *L*-coefficient of variation and *L*-skewness for eight catchments in Tasmania (region 3) and seven catchments in Western Australia (region 6) which are dominated by rainfall during the winter months.

floodflow data in the winter-dominated rainfall regimes and the GPA distribution provides a good approximation in the remaining regions.

Different flood frequency models for different hydrologic regions

Considering the evidence provided in Fig. 6 and in Pearson et al. (1991) and Nathan and Weinmann (1991), one questions whether a single flood frequency model is suitable for the entire continent of Australia. One could employ the quantitative discordancy and heterogeneity measures introduced

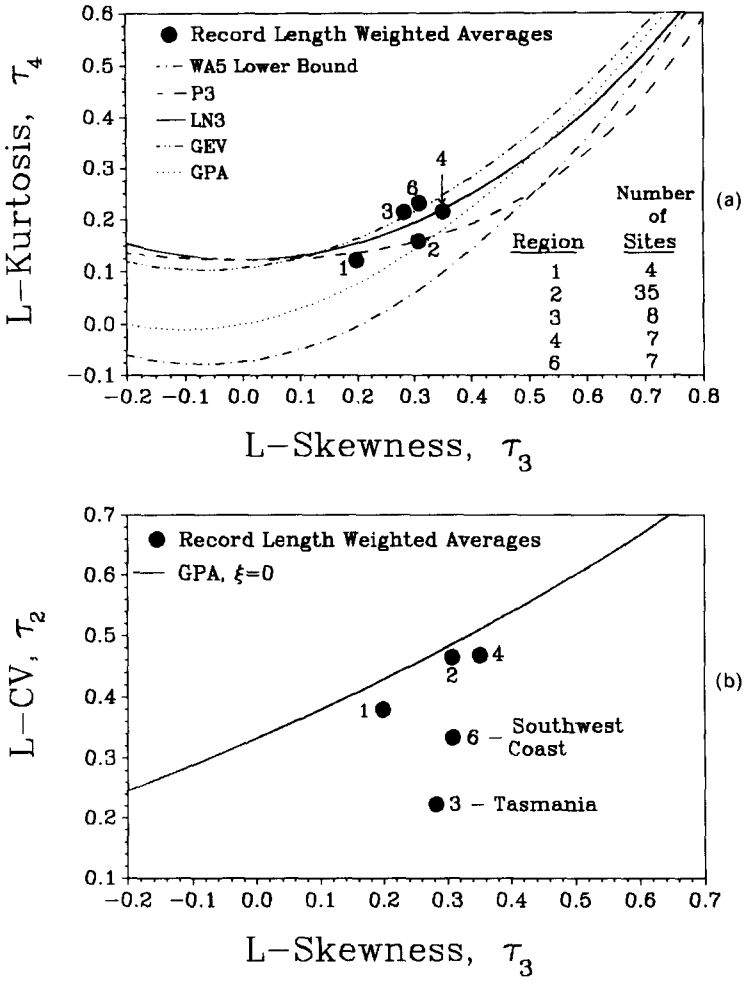

Fig. 7. *L*-moment diagrams comparing the sample record length weighted averages for each region with theoretical relationships for (a) *L*-kurtosis and *L*-skewness of floodflows and (b) *L*-coefficient of variation and *L*-skewness of floodflows. The numbers next to each point denote the region number.

by Hosking and Wallis (1993) to evaluate which regions of Australia are hydrologically homogeneous.

Rather than explaining and employing the procedures advocated by Hosking and Wallis (1993), we elected to compute the record length weighted average of L-C_v, L-skewness and L-kurtosis for each of the major Australian drainage divisions considered here. The results are illustrated in Fig. 7, where the number next to each point denotes the drainage region described in Fig. 1. Figure 7(b) confirms again, that the basins in the winter-dominated rainfall

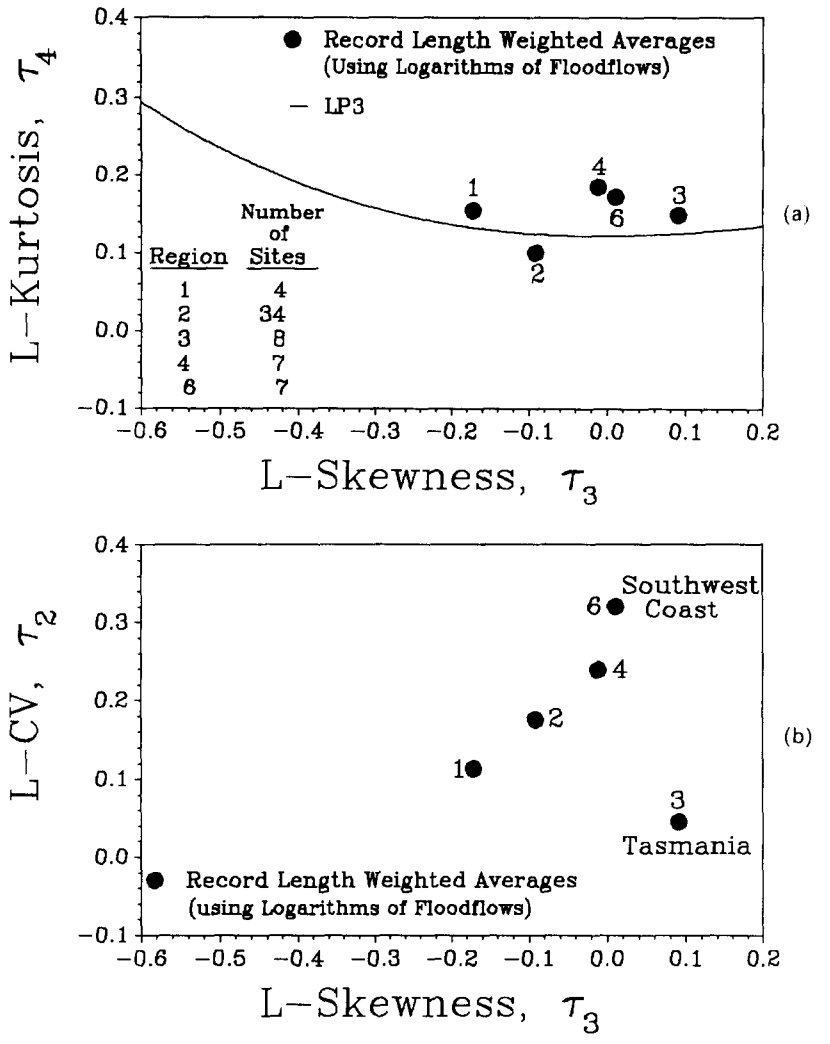

Fig. 8. *L*-moment diagrams comparing the sample record length weighted averages for each region with theoretical relationships for (a) *L*-kurtosis and *L*-skewness of natural logarithms of streamflow and (b) *L*-coefficient of variation and *L*-skewness of natural logarithms of floodflows. The numbers next to each point denote the region number.

regime (southwest coast and Tasmania) behave quite differently from the remaining Australian basins. Figure 7(a) documents that the record length weighted average values of *L*-skewness and *L*-kurtosis for the winter-dominated rainfall regimes (regions 3 and 6) fall on the theoretical GEV curve. Most of the remaining sites (35 sites in the southeast coastal region; region 2) fall close to the theoretical GPA curve. Even though the record length weighted average *L*-moments for regions 1 and 2 fall very close to the

theoretical P3 relationships, we recall from Fig. 3 that the P3 model provides a poor representation of the distribution of floodflows for all regions considered.

We conclude from Fig. 7, that the GPA distribution should provide a good approximation to the distribution of floodflows in the southeast coastal region, which is the most densely populated region of Australia. We also conclude from Fig. 7 that the GEV distribution provides a good approximation to the distribution of floodflows in the winter-dominated rainfall regions; southwest coastal region (region 6), Tasmania (region 3), and portions of the Murray–Darling basin (region 4).

Figure 8, like Fig. 7, illustrates record length weighted averages for each river basin, however, Fig. 8 depicts L-moments of the natural logarithms of the floodflows. Figure 8(a) demonstrates, as does Fig. 4, that the LP3 distribution provides a reasonably good approximation to the distribution of floodflows throughout the regions of Australia considered here. Figure 8(b) shows again that the southwest coastal region and Tasmania behave hydrologically quite different from the remainder of Australia. On the one hand, these two regions are similar because they are dominated by rainfall during the winter months. Yet these two regions are shown in Fig. 8(b) to have dramatically different values of L-C_v in log space. This is to be expected since Tasmania receives much higher rainfall than the southwest coastal region. We conclude from Fig. 8 that the LP3 distribution, currently adopted in Australia, provides a reasonable approximation to the distribution of floodflows for all regions of Australia considered here.

NON-PARAMETRIC EVALUATION OF FLOOD FREQUENCY PROCEDURES

The previous comparisons focused on the ability of alternate probability models to approximate the distribution of floodflows, however, those comparisons did not evaluate the ability of alternate methods to provide estimates of design quantiles. In this section we evaluate the performance of alternate models and parameter estimation schemes in terms of their ability to predict the 100 year floodflow. We repeat a portion of the experiment performed by Beard (1974) and summarized in IACWD (1982), which led to the original uniform flood frequency guidelines in the US. The experiment is conceptually simple and focuses on the important question of how well each model and associated parameter estimation scheme perform in terms of predicting extreme floodflows with a fixed annual exceedance probability.

Floodflow frequency methods evaluated

The experiment begins by estimating the 100 year floodflow at each of the 61 sites using the following at-site methods.

Log Pearson type 3 distribution (LP3)

The method-of-moments in log space, as recommended by Pilgrim (1987) and IACWD (1982) is always used for estimating the mean, variance and skewness of the logarithms. We do not consider the use of a weighted skew coefficient, as recommended in practice by Pilgrim (1987) and IACWD (1982), because that procedure would be a regional procedure and all of our comparisons are limited to at-site procedures.

Log–normal distribution

Two procedures are considered. The two-parameter log–normal procedure (LN2) employs maximum likelihood estimators and the three-parameter log–normal procedure (LN3) employs Stedinger's (1980) estimator of the lower bound ξ along with sample estimates of the mean and variance of $y_i = \ln(x_i - \xi)$, where the x_i are the observed floodflows. Stedinger (1980) and Stedinger et al. (1993) summarize these procedures.

Generalized Extreme Value distribution

The generalized extreme value procedure (GEV) employs unbiased L-moment estimators of each distribution's parameters as described in Stedinger et al. (1993) and Hosking (1990).

Generalized Pareto distribution

The Generalized Pareto procedure (GPA) employs the unbiased L-moment estimators of its three parameters as described in the Appendix.

Expected probability adjustment

Most quantile estimators provide almost unbiased estimates of the percentile of interest. Hence one expects, on average, the estimated 100 year event to equal its population value. However, an unbiased estimator of the T year event will not, in general, be exceeded with an average probability of $p = 1/T$. Beard (1960, 1978), IACWD (1982, appendix 11), Gunasekara and Cunnane (1991) and Stedinger et al. (1993) discuss this issue in greater detail.

For normal and log–normal samples, Pilgrim (1987, section 10.6) provides tables and Bulletin 17B (IACWD, 1982, appendix 11) provides formulae for the probabilities that an almost unbiased quantile estimator of the T year

TABLE 2

The number of observed floodflows that exceed the 100 year floodflow computed from each station's complete record using five different methods with an expected probability adjustment

Method	Number of exceedances X		
	All sites	Only region 2	All sites except regions 3 and 6
LP3	13[a]	4	8
LN3	13[a]	5	8
LN2	16[a]	4	7
GEV	17[a]	9[a]	12[a]
GPA	26[a]	14[a]	18[a]
Total no. of sites	60	34	45
Total site-years	1936	1208	1497
Theoretical expectation	19	12	15
90% likely interval $[X_{0.05}, X_{0.95}]$	(13, 26)	(7, 17)	(9, 21)

[a] Denotes results that fall inside 90% likely interval.

event will be exceeded. For example, for the $T = 100$ year event the expected annual exceedance probability is $0.01(1.0+26/N^{1.16})$. Note that for the average sample size employed here ($N = 32$ years), the expected exceedance probability for the $T = 100$ year event is 0.0147, instead of 0.01. Thus, a design for the $T = 100$ year event, will lead to floods exceeded on average every $T = 68$ years. Although these corrections were derived for the normal and log-normal distributions, they have been recommended by IACWD (1982) for use with the LP3 distribution. We employ these corrections for all of the methods considered. Gunasekara and Cunnane (1991) showed that the expected probability correction for normally distributed samples employed here, is approximately valid for other distributions.

Experimental procedure

Using each of the above five methods, we counted the number of times an observed annual maximum floodflow, at each site, exceeded the estimated $T = 100$ year floodflow using an expected probability adjustment. The results are reported in Table 2. If one assumes that the sites are independent and that floods occur independently from one year to the next, at each site, then the number of exceedances, X, follows a binomial distribution with mean $E[X] = np$ and variance $\mathrm{Var}[X] = np(1-p)$, where n is the number of independent trials and p is the exceedance probability associated with each event ($p = 1/T$).

For example, across the 60 sites employed (one site is dropped due to a zero flow), there are $n = 1936$ site-years of data (or independent trials). On average, over many such experiments, one expects to observe approximately $E[X] = 19$ exceedances of the 100 year event. Furthermore, since X follows a binomial distribution we can estimate the 90% likely interval as the range of values one might expect, 90% of the time, over repeated experiments of this kind. The 90% interval $(x_{0.05}, x_{0.95})$ is reported in Table 2 and found from

$$0.90 = \sum_{x=x_{0.05}}^{x_{0.95}} \binom{n}{x} p^x (1-p)^{n-x} \tag{7}$$

where $n = 1936$ and $p = 0.01$.

RESULTS

Table 2 reports the number of observed floodflows, out of the entire sample of 1936 site-years of floodflows, which exceeded the 100 year event. We document the results corresponding to five different quantile estimation methods. The experiment is repeated three times, first with all 60 sites, next using only the 35 sites in the southeast coastal region (region 2) and finally for all sites except those in Tasmania (basin 3) and southwest coastal region (region 6). The only procedures which led to observed exceedances that always fell within the 90% likely interval are the GEV and GPA procedures.

Table 2 reveals that all five procedures led to observed exceedances that fall within the 90% likely interval when one considers all 60 sites, however the GEV and LN2 procedures came closest to the theoretical expectation. One might expect all these procedures to perform credibly, given the large scatter shown in Fig. 3(a), and our earlier conclusions based on Figs. 3, 4 and 5. The LN2 and GEV procedures best reproduced the theoretically expected number of exceedances for all sites (19 exceedances) due to the robustness of those procedures. Vogel et al. (1993) obtained similar results using 383 sites in the southwestern United States.

When we only employ the 35 southeast coastal catchments (region 2), Table 2 documents that the GPA distribution reproduces, almost exactly, the theoretically expected number of exceedances. This result is to be expected from Fig. 7(a) where we showed that the record length weighted average L-moment ratios for this region fell on the GPA theoretical curve. This result supports our prior recommendation to employ the GPA distribution for modeling floodflows in the most populated region of Australia, the southeast coastal region.

When one employs the 45 catchments that are not located in the winter-dominated rainfall regions (regions 3 and 6), again the GEV and GPA

procedures are the only procedures that reproduce the theoretically expected number of exceedances. Again one would have expected the GPA distribution to perform credibly, since we showed earlier in Figs. 3, 5 and 7 that the GPA distribution provides a good approximation to sample L-moment ratios for all regions except the winter-dominated rainfall regions. One may not have predicted the GEV distribution to perform satisfactorily here since it performed poorly for basins 1, 2 and 4 in Fig. 7(a), hence we suspect that this result is due again to the robustness of the GEV procedures.

Unfortunately, experiments such as the one reported in Table 2, can never be definitive because actual floodflow samples are cross-correlated in space. Cross-correlation reduces the amount of regional experience, implying that one needs more basins to obtain convergence between the theoretical number of exceedances and the observed number of exceedances. To obtain more definitive results one needs to employ hundreds of basins, similar to the studies by Beard (1974), Gunasekara and Cunnane (1992) and Vogel et al. (1993).

Interestingly, Gunasekara and Cunnane (1992) reached almost identical conclusions to ours by repeating Beard's experiment with synthetic floodflow data. Gunasekara and Cunnane (1992) generated 40 year synthetic floodflow traces at 300 artificial sites from seven different parent probability distributions. They employed 13 different model/parameter estimation procedures to estimate the 10, 100 and 1000 year floodflow at each site. They found that for both the 100 and 1000 year events, the regional LP3 procedures advocated by IACWD (1982) and Pilgrim (1987) (which use regional skew estimates) and the GEV procedures employed here, reproduced the expected number of exceedances better than any of the procedures they evaluated. These results are similar to ours except we also found that the LN2, LN3 and GPA procedures performed well. Gunasekara and Cunnane (1992) did not consider the GPA and LN3 procedures and the reason they rejected the LN2 procedure was probably due to the fact that the average skewness of the logarithms of their artificial samples was significantly different from zero. The average L-skewness of the logarithms of the floodflow data at all 60 sites used here was -0.06. This fact taken together with Fig. 7(a) document why the LN2 procedure performed so well in this study.

The at-site LP3 method did not perform well in all regions because such procedures are highly dependent upon our ability to estimate skewness and small sample estimates of the skew coefficient are known to be highly imprecise. It is likely that the use of a weighted skew coefficient as recommended by IACWD (1982) and Pilgrim (1987) would have improved its performance.

CONCLUSIONS

The primary objective of this study was to select a set of suitable probability distributions for modeling annual maximum floodflows in Australia. *L*-moment diagrams revealed that the Generalized Pareto (GPA), log Pearson type 3 (LP3), three-parameter log–normal (LN3), Generalized Extreme Value (GEV), and Wakeby (WA5) distributions all provide acceptable approximations to the distribution of floodflows in Australia. Of all the models evaluated, Figs. 3, 4, 7 and 8 reveal that the GPA and LP3 distributions probably provide the best description of the distribution of floodflows across the entire continent of Australia, however, further analysis revealed that separation of Australia into broad homogeneous regions can improve our ability to discriminate among potential flood frequency models such that the GPA distribution provides the best approximation to the distribution of floodflows in the most densely populated regions of the southeastern coastal region (region 2). Of the models tested, the GEV distribution provides the best approximation to the distribution of floodflows in the winter-dominated rainfall regions of Tasmania and the southwest coast (see Fig. 1). In addition, Figs. 3, 4, 7 and 8 revealed that the LN3 and the LP3 distributions also perform credibly across all regions considered. Figures 2 and 3 revealed that the Pearson type 3 (P3), normal, Gumbel, uniform and exponential distributions perform poorly.

To assess the ability of alternate flood frequency models and parameter estimation schemes to estimate design quantiles we also repeated a portion of the original non-parametric experiment performed by Beard (1974) which led to the Water Resource Council (IACWD, 1982) and Institution of Engineers' (Pilgrim, 1987) decisions to recommend the LP3 procedures in the United States and Australia, respectively. Those experiments document again that if one had to select a single model for all regions of Australia considered here, then the GPA, LN3, LN2, LP3 and GEV procedures are all acceptable alternatives. However, both the GPA and GEV procedures appear to be preferred for modeling floodflows for regions outside the winter-dominated rainfall regime. The GEV procedures seem to perform well for all regions considered, in spite of the fact that the *L*-moment diagrams do not always favor the GEV procedure (see Fig. 3(a)). These conclusions are surprisingly similar to the results of a recent study by Gunasekara and Cunnane (1992).

It is indeed satisfying to report that all our evaluations consistently reach similar conclusions. Yet these results do not imply that the current IACWD (1982) and Institution of Engineers (Pilgrim, 1987) guidelines are satisfactory. Recent studies by Potter and Lettenmaier (1990) and others demonstrate that regional index-flood procedures for the GEV distribution with *L*-moment

estimators should be more accurate and more robust than the type of at-site procedures described here and recommended by IACWD (1982). Stedinger et al. (1993) provide a summary of index-flood procedures. Nevertheless, this study reveals that index-flood procedures need not be restricted to the GEV distribution because the GPA distribution appears to provide a better representation of floodflow data in the most densely populated regions of Australia.

Finally, we emphasize, as Potter (1987) and others have, that improvements in regional flood frequency analysis must be derived from the type of at-site procedures evaluated here, because the single-site model lies at the heart of all regional procedures. Hopefully, future investigations in Australia will employ a significantly larger sample of floodflow data so that more definitive conclusions may be reached for regions of Australia that were not included in this study and for regions where streamgauge densities were low (see Fig. 1).

ACKNOWLEDGMENTS

We are grateful to Michael Hynes for the assistance he provided with a portion of the computer programming. This research was supported by the Center for Environmental Applied Hydrology at the University of Melbourne and the Department of Civil Engineering at Tufts University, and was completed while the first author was on sabbatical leave in Melbourne. The streamflow data were obtained from the Queensland Water Resources Commission, the Department of Water Resources of New South Wales, the Rural Water Commission of Victoria, the Hydro Electric Commission of Tasmania and the Western Australia Water Authority.

REFERENCES

Beard, L.R., 1960. Probability estimates based on small normal-distribution samples. J. Geophys. Res., 65(7): 2143–2148.

Beard, L.R., 1974. Flood Flow Frequency Techniques. Center for Research in Water Resources, The University of Texas at Austin.

Beard, L.R., 1978. Impact of hydrologic uncertainties on flood insurance. J. Hydraul. Div., ASCE, 104(HY11): 1473–1483.

Benson, M.A., 1968. Uniform flood-frequency estimating methods for federal agencies. Water Resour. Res., 4(5): 891–908.

Chowdhury, J.U., Stedinger, J.R. and Lu, L., 1991. Goodness-of-fit tests for regional GEV flood distributions. Water Resour. Res., 27(7): 1765–1776.

Cunnane, C., 1989. Statistical distributions for flood frequency analysis. Operational Hydrology Rep. No. 33, WMO No. 718, Appendix 3, World Meteorological Organization, Geneva.

Fitzgerald, D.L., 1989. Single station and regional analysis of daily rainfall extremes. Stochastic Hydrol. Hydraul., 3: 281–292.

Greenwood, J.A., Landwehr, J.M., Matalas, N.C. and Wallis, J.R., 1979. Probability weighted moments: definition and relation to parameters of several distributions expressible in inverse form. Water Resour. Res., 15(5): 1049–1054.

Gunasekara, T.A.G. and Cunanne, C., 1991. Expected probabilities of exceedance of normal flood distributions. J. Hydrol., 128: 101–113.

Gunasekara, T.A.G. and Cunanne, C., 1992. Split sampling technique for selecting a flood frequency analysis procedure. J. Hydrol., 130: 189–200.

Hosking, J.R.M., 1990. L-moments: analysis and estimation of distributions using linear combinations of order statistics. J. R. Stat. Soc., B, 52(2): 105–124.

Hosking, J.R.M., 1991a. Approximations for use in Constructing L-moment ratio diagrams. Research Rep. RC-16635, IBM Research Division, T.J. Watson Research Center, Yorktown Heights, NY, 3 pp.

Hosking, J.R.M., 1991b. Fortran routines for use with the method of L-moments, Version 2. Research Rep. RC-17097, IBM Research Division, T.J. Watson Research Center, Yorktown Heights, NY, 117 pp.

Hosking, J.R.M. and Wallis, J.R., 1987. Parameter and quantile estimation for the Generalized Pareto distribution. Technometrics, 29(3): 339–349.

Hosking, J.R.M. and Wallis, J.R., 1993. Some statistics useful in regional frequency analysis. Water Resour. Res., 29(2): 271–281.

Interagency Advisory Committee on Water Data (IACWD), 1982. Guidelines for determining flood flow frequency. Bulletin 17B of the Hydrology Subcommittee, OWDC, US Geological Survey, Reston, VA.

Jain, D. and Singh, V.P., 1987. Estimating parameters of EVI distribution for flood frequency analysis. Water Resour. Bull., 23(1): 59–71.

Landwehr, J.M., Matalas, N.C. and Wallis, J.R., 1979. Probability weighted moments compared with some traditional techniques in estimating parameters and quantities. Water Resour. Res., 15(5): 1055–1064.

McMahon, T.A. and Srikanthan, R., 1981. Log Pearson III distribution — is it applicable to flood frequency analysis of Australian streams? J. Hydrol., 52: 139–147.

Nathan, R.J. and Weinmann, P.E., 1991. Application of at-site and regional flood frequency analyses. In: Proc. Int. Hydrology Water Resources Symp., Perth, 2–4 October. pp. 769–774.

Pearson, C.P., 1992. New Zealand regional flood frequency analyses using L-moments. In: Proc. 12th Conf. on Probability and Statistics in the Atmospheric Sciences, 5th Int. Meeting on Statistical Climatology, Toronto, 22–26 June 1992.

Pearson, C.P., McKerchar, A.I. and Woods, R.A., 1991. Regional flood frequency analysis of Western Australian data using L-moments. In: Proc. Int. Hydrology & Water Resources Symp., Perth, 2–4 October 1991. pp. 631–632.

Pickands, J., 1975. Statistical inference using extreme order statistics. Ann. Stat., 3: 119–131.

Pilgrim, D.H. (Editor), 1987. Australian Rainfall and Runoff, A Guide to Flood Estimation, Vol. I. The Institution of Engineers, Barton ACT, Australia.

Potter, K.W., 1987. Research on flood frequency analysis: 1983–1986. Rev. Geophys., 25(25): 113–118.

Potter, K.W. and Lettenmaier, D.P., 1990. A comparison of regional flood frequency estimation methods using a resampling method. Water Resour. Res., 26(3): 415–424.

Stedinger, J.R., 1980. Fitting lognormal distributions to hydrologic data. Water Resour. Res., 16(3): 481–490.

Stedinger, J.R., Vogel, R.M. and Foufoula-Georgiou, E., 1993. Frequency analysis of extreme

events. In: D. Maidment (Editor), Handbook of Applied Hydrology. Mc-Graw Hill Book Co., New York, Chapter 18.
U.S. Water Resources Council, 1967. Guidelines for determining flood flow frequency. Bulletin 15, Hydrol. Comm., Washington, DC (also see Interagency Advisory Committee on Water Data, 1982).
Vogel, R.M., 1986. The probability plot correlation coefficient test for the normal, lognormal and Gumbel distributional hypothesis. Water Resour. Res., 22(4): 587–590. Correction: Water Resour. Res., 23(10) 2013 (1987).
Vogel, R.M. and Kroll, C.N., 1989. Low-flow frequency analysis using probability-plot correlation coefficients. J. Water Resour., Planning Manage., ASCE, 115(3): 338–357.
Vogel, R.M. and McMartin, D.E., 1991. Probability plot goodness-of-fit and skewness estimation procedures for the Pearson type 3 distribution. Water Resour. Res., 27(12): 3149–3158.
Vogel, R.M., Thomas, W.O. and McMahon, T.A., 1993. Floodflow frequency model selection in Southwestern U.S.A. J. Water Resour., Planning Manage., ASCE, 119(3): in press.
Wallis, J.R., 1988. Catastrophes, computing and containment: living in our restless habitat. Speculation Sci. Technol., 11(4): 294–315.
Wallis, J.R., Matalas, N.C. and Slack, J.R., 1974. Just a moment. Water Resour. Res., 10(2): 211–219.

APPENDIX: GENERALIZED PARETO DISTRIBUTION

The Pareto distribution was first introduced in the field of economics by Vilfredo Pareto for modeling the distribution of income above a threshold. Subsequently the Generalized Pareto distribution (GPA) introduced by Pickands (1975) has been applied to rainfall depths (Fitzgerald, 1989) and floodflows (Hosking and Wallis, 1987). Hosking and Wallis (1987), Stedinger et al. (1993) and others show that when floodflows above a threshold follow a GPA distribution and the number of floodflows above the threshold follow a Poisson distribution, then the annual maximum floodflows follow a GEV distribution. Hence the GPA distribution provides an important linkage between the theory of annual maximum floodflow series and partial-duration series.

The theoretical properties of the Generalized Pareto distribution

Hosking and Wallis (1987) describe the theoretical properties of the two-parameter GPA distribution. They show that if Q follows a GPA distribution then $Q-\xi$ also follows a GPA distribution as long as $Q \geqslant \xi$. This fact can be used to extend the two-parameter GPA distribution to a three-parameter distribution as is done in this section. The three-parameter GPA distribution has pdf

$$f_Q(q) = \alpha^{-1}[1-k(q-\xi)/\alpha]^{(1/k-1)} \qquad k \neq 0 \qquad \text{(A1a)}$$

$$= \alpha^{-1} \exp[-(q-\xi)/\alpha] \qquad k = 0 \qquad \text{(A1b)}$$

and cdf

$$F_Q(q) = 1-[1-k(q-\xi)/\alpha]^{1/k} \qquad k \neq 0 \tag{A2a}$$

$$= 1-\exp[(q-\xi)/\alpha] \qquad k = 0 \tag{A2b}$$

For $k \leqslant 0$ streamflow is bounded below so that $\xi \leqslant Q \leqslant \infty$. For $k > 0$, streamflow is bounded both above and below so that $\xi \leqslant Q \leqslant (\xi+\alpha/k)$. When $\xi = 0$ and $k = 0$, the GPA distribution reduces to the exponential distribution. When $\xi = 0$ and $k = 1$, the GPA distribution reduces to the uniform distribution (see Fig. 2).

The GPA distribution parameters can be related to conventional product moments (Hosking and Wallis, 1987), *L*-moments (Hosking, 1990; Stedinger et al., 1992) and probability weighted moments (Hosking and Wallis, 1987). If they exist, the mean, variance, skewness and kurtosis are, respectively,

$$\mu = \xi+\alpha/(1+k) \tag{A3a}$$

$$\sigma^2 = \alpha^2/[(1+k)^2(1+2k)] \tag{A3b}$$

$$\gamma = 2(1+2k)^{1/2}(1-k)/(1+3k) \tag{A3c}$$

and

$$\kappa = \frac{3+(1+2k)(3-k+2k^2)}{(1+3k)(1+4k)} - 3 \tag{A3d}$$

The distribution has infinite variance, skewness and kurtosis for $k \leqslant -1/2$, $k \leqslant -1/3$ and $k \leqslant -1/4$, respectively. The values of ξ, α and k written in terms of *L*-moments are

$$k = (1-3\tau_3)/(1+\tau_3) \tag{A4a}$$

$$\alpha = \lambda_2(1+k)(2+k) \tag{A4b}$$

$$\xi = \lambda_1-\alpha/(1+k) \tag{A4c}$$

where λ_r, $r = 1$, 2 and 3 are the first three *L*-moments.

Quantile estimation using the Generalized Pareto distribution

The cdf of the GPA distribution is easily inverted to obtain the quantile function

$$Q_p = \xi+(\alpha/k)[1-p^k] \tag{A5}$$

where p is the annual exceedance probability and Q_p is that value of streamflow which is exceeded with probability p. A sample quantile based on *L*-moment estimators is easily obtained by substituting sample estimates of λ_r,

$r = 1, \ldots, 3$, into eqns. (A4) and (A5). L-moment estimators are relatively simple to compute and always produce feasible values for the estimated parameters. Hosking and Wallis (1987) compared the efficiency of quantile estimators based on PWM, method-of-moments and maximum likelihood estimates of α and k with ξ set to zero.

L-moment relationships for the Generalized Pareto distribution

Hosking (1990) derived relationships between the L-moments and the GPA model parameters

$$\lambda_1 = \xi + \alpha/(1+k) \tag{A6a}$$

$$\lambda_2 = \alpha/[(1+k)(2+k)] \tag{A6b}$$

$$\tau_3 = (1-k)/(3+k) \tag{A6c}$$

$$\tau_4 = (1-k)(2-k)/[(3+k)(4+k)] \tag{A6d}$$

where τ_4 and τ_3 are defined in (6). Hosking (1991a) also derived an approximate relationship between L-kurtosis and L-skewness, useful for comparing the theoretical L-moment relationships with sample estimates

$$\tau_4 = 0.20196\tau_3 + 0.95924\tau_3^2 - 0.20096\tau_3^3 + 0.04061\tau_3^4 \tag{A7}$$

An L-moment diagram for the GPA distribution that illustrates the relationship between τ_4 and τ_3, depends only upon the important shape parameter k, similar to the GEV distribution.